# Promiscuous phosphoketolase and metabolic rewiring enables novel non-oxidative glycolysis in yeast for high-yield production of acetyl-CoA derived products

Downloaded from: https://research.chalmers.se, 2021-08-31 11:42 UTC

Citation for the original published paper (version of record):
Hellgren, J., Godina, A., Nielsen, J. et al (2020)
Promiscuous phosphoketolase and metabolic rewiring enables novel non-oxidative glycolysis in yeast for high-yield production of acetyl-CoA derived products
Metabolic Engineering, 62: 150-160
http://dx.doi.org/10.1016/j.ymben.2020.09.003

N.B. When citing this work, cite the original published paper.

research.chalmers.se offers the possibility of retrieving research publications produced at Chalmers University of Technology.
It covers all kind of research output: articles, dissertations, conference papers, reports etc. since 2004.
research.chalmers.se is administrated and maintained by Chalmers Library

(article starts on next page)

Metabolic Engineering 62 (2020) 150–160

Contents lists available at ScienceDirect

Metabolic Engineering

journal homepage: www.elsevier.com/locate/meteng

# Promiscuous phosphoketolase and metabolic rewiring enables novel non-oxidative glycolysis in yeast for high-yield production of acetyl-CoA derived products

John Hellgren [a,b], Alexei Godina [c], Jens Nielsen [a,b,d], Verena Siewers [a,b,*]

[a] Department of Biology and Biological Engineering, Chalmers University of Technology, Gothenburg, Sweden
[b] Novo Nordisk Foundation Center for Biosustainability, Chalmers University of Technology, Gothenburg, Sweden
[c] TOTAL S.A., Refining & Chemicals, Strategy Development & Research, Biofuels Division, Courbevoie, France
[d] BioInnovation Institute, Ole Maaløes Vej 3, DK2200, Copenhagen N, Denmark

ARTICLE INFO

*Keywords:*
3-Hydroxypropionic acid
Mathematical modelling
Metabolic engineering
Non-oxidative glycolysis
*Saccharomyces cerevisiae*
Synthetic biology

ABSTRACT

Carbon-conserving pathways have the potential of increasing product yields in biotechnological processes. The aim of this project was to investigate the functionality of a novel carbon-conserving pathway that produces 3 mol of acetyl-CoA from fructose-6-phosphate without carbon loss in the yeast *Saccharomyces cerevisiae*. This cyclic pathway relies on a generalist phosphoketolase (Xfspk), which can convert xylulose-5-phosphate, fructose-6-phosphate and sedoheptulose-7-phosphate (S7P) to acetyl phosphate. This cycle is proposed to overcome bottlenecks from the previously reported non-oxidative glycolysis (NOG) cycle. Here, *in silico* simulations showed accumulation of S7P in the NOG cycle, which was resolved by blocking the non-oxidative pentose phosphate pathway and introducing Xfspk and part of the riboneogenesis pathway. To implement this, a transketolase and transaldolase deficient *S. cerevisiae* was generated and a cyclic pathway, the **G**lycolysis **A**l**T**ernative **H**igh **C**arbon **Y**ield **C**ycle (GATHCYC), was enabled through *xfspk* expression and sedoheptulose bisphosphatase (*SHB17*) overexpression. Flux through the GATHCYC was demonstrated *in vitro* with a phosphoketolase assay on crude cell free extracts, and *in vivo* by constructing a strain that was dependent on a functional pathway to survive. Finally, we showed that introducing the GATHCYC as a carbon-conserving route for 3-hydroxypropionic acid (3-HP) production resulted in a 109% increase in 3-HP titers when the glucose was exhausted compared to the phosphoketolase route only.

## 1. Introduction

The native routes for carbon conversion in microorganisms have been optimized through evolution, but not always in a way that is optimal for bioproduction of valuable products. In metabolic engineering, the metabolic network of a cell is optimized to increase the fluxes towards the product of interest, with the goal of improving the **T**iter, **R**ate and **Y**ield (TRY) metrices (Nielsen and Keasling, 2016). The yeast *Saccharomyces cerevisiae* is an attractive industrial production host due to the robustness of the organism, ease of genetic manipulation and a vast knowledgebase being available (Nielsen and Jewett, 2008). *S. cerevisiae* is a Crabtree positive yeast (De Deken, 1966), which means that it will exhibit fermentative growth when glucose is in excess, even in aerobic conditions, with ethanol as the main product. When the glucose is consumed (marking the end of the glucose phase), the diauxic shift occurs, where *S. cerevisiae* reprograms its metabolism from fermentative growth to respiratory growth on ethanol. The growth on the produced ethanol is usually referred to as the ethanol phase.

A key precursor metabolite for numerous industrially relevant products is acetyl coenzyme A (acetyl-CoA), whose bioconversion into different products can be enhanced by increasing its supply (Nielsen, 2014). When an efficient platform strain (Rodriguez et al., 2015) with high flux towards acetyl-CoA has been established, it can be used as a starting point for creating strains producing any product derived from acetyl-CoA. Most biosynthetic pathways are located in the cytosol, which means that the production of cytosolic acetyl-CoA needs to be increased as acetyl-CoA cannot be transported freely between the compartments in *S. cerevisiae*. The native route for cytosolic acetyl-CoA

* Corresponding author. Department of Biology and Biological Engineering, Chalmers University of Technology, Kemivägen 10, SE412 96, Gothenburg, Sweden.
*E-mail address:* siewers@chalmers.se (V. Siewers).

https://doi.org/10.1016/j.ymben.2020.09.003
Received 3 June 2020; Received in revised form 11 August 2020; Accepted 3 September 2020
Available online 8 September 2020
1096-7176/© 2020 The Author(s). Published by Elsevier Inc. on behalf of International Metabolic Engineering Society. This is an open access article under the CC BY license (http://creativecommons.org/licenses/by/4.0/).

production in *S. cerevisiae* is the pyruvate dehydrogenase (PDH) bypass, consisting of pyruvate decarboxylase, acetaldehyde dehydrogenase and acetyl-CoA synthetase. Successful strategies in improving the cytosolic acetyl-CoA supply have been achieved by optimizing this native cytosolic pathway (Chen et al., 2014), however, a drawback with this pathway is the net cost of 1 ATP per acetyl-CoA formed from ½ glucose. This cost of ATP can negatively impact the yields of cytosolic acetyl-CoA derived products from glucose. Therefore, several successful strategies using heterologous pathways to provide cytosolic acetyl-CoA have been implemented (van Rossum et al., 2016). A widely used strategy involves transporting mitochondrial acetyl-CoA to the cytosol with the citrate-oxaloacetate shuttle, involving mitochondrial citrate synthase, citrate-α-ketoglutarate antiporter (Yhm2) and ATP-citrate lyase (Yu et al., 2018; Zhu et al., 2020). Furthermore, acetate formation and ATP cost in the PDH bypass can be avoided by converting acetaldehyde directly to acetyl-CoA by acetylating acetaldehyde dehydrogenase (Kozak et al., 2014a). Successful attempts have also been made to express the PDH complex from *Enterococcus faecalis* in the yeast cytosol (Kozak et al., 2014b). The main downside of most of these strategies is the loss of carbon as $CO_2$, which decreases the theoretical product yield and the profitability of the process. Obtaining high yields is important as substrate costs may cover up to 75% of the total process costs (Lynd et al., 1999).

An interesting enzyme in this respect is phosphoketolase, which can irreversibly convert fructose-6-phosphate (F6P) or xylulose-5-phosphate (X5P) to acetyl-phosphate (AcP) and erythrose-4-phosphate (E4P) or glyceraldehyde-3-phosphate (GAP). Dual activity towards both F6P and X5P is found for the bifidobacterial enzyme, where it is part of the bifid shunt (Suzuki et al., 2010). Phosphoketolase can be coupled to the enzyme phosphotransacetylase (Pta), which catalyzes the reversible reaction between AcP and acetyl-CoA, forming an attractive route for increased acetyl-CoA supply without any carbon loss. The phosphoketolase pathway has been successfully deployed in yeast for polyhydroxybutyrate (Kocharin et al., 2013), fatty acid ethyl ester (de Jong et al., 2014) and farnesene (Meadows et al., 2016) production. The best performing strain for farnesene utilized a combination of a carbon-wasting but ATP and reducing power producing pathway, and a phosphoketolase-based carbon-saving pathway that however did not produce ATP or reducing power.

Phosphoketolase is the key enzyme in the fructose-6-phoshate shunt (Schramm and Racker, 1957), which through carbon rearrangement can convert 1 mol of F6P to 3 mol of AcP without any loss of carbon, thus with a high potential of increasing yields. This cycle, nowadays referred to as non-oxidative glycolysis (NOG), is shown in Fig. 1A and has been utilized in *Escherichia coli* to convert xylose (Bogorad et al., 2013) and glucose (Lin et al., 2018) at near theoretical yields to acetate. However, there might be a possible bottleneck in this configuration as NOG involves several reactions requiring two substrates (transaldolase and transketolase).

Two new variants of the NOG pathway (Fig. 1B–C) have been proposed through mathematical modelling by Andersen et al. (2019). These are made possible through a novel phosphoketolase activity towards sedoheptulose-7-phosphate (S7P). The first variant (Fig. 1B) was recently demonstrated to have *in vivo* activity in *E. coli* by Krüsemann et al. (2018). The authors used the phosphoketolase from *Bifidobacterium adolescentis*, which was shown to act upon X5P, F6P and S7P (Xfspk), and named the cycle the phosphoketolase shunt. This cycle does not require the transketolase step. The second variant of the NOG pathway proposed by Andersen et al. (2019) is shown in Fig. 1C, here named the **G**lycolysis **AlT**ernative **H**igh **C**arbon **Y**ield **C**ycle (GATHCYC) and will be evaluated in this paper. This cycle uses Xfspk from *Bifidobacterium longum*, which also has been shown to have activity on S7P (Beck et al., 2015), and does not include a transketolase or transaldolase step. All genes required, except the phosphoketolase, are already present in the *S. cerevisiae* genome. The sedoheptulose-1,7-bisphosphate aldolase (Sba) reaction is catalyzed by Fba1 and the sedoheptulose-1,7-bisphosphatase (Sbp)

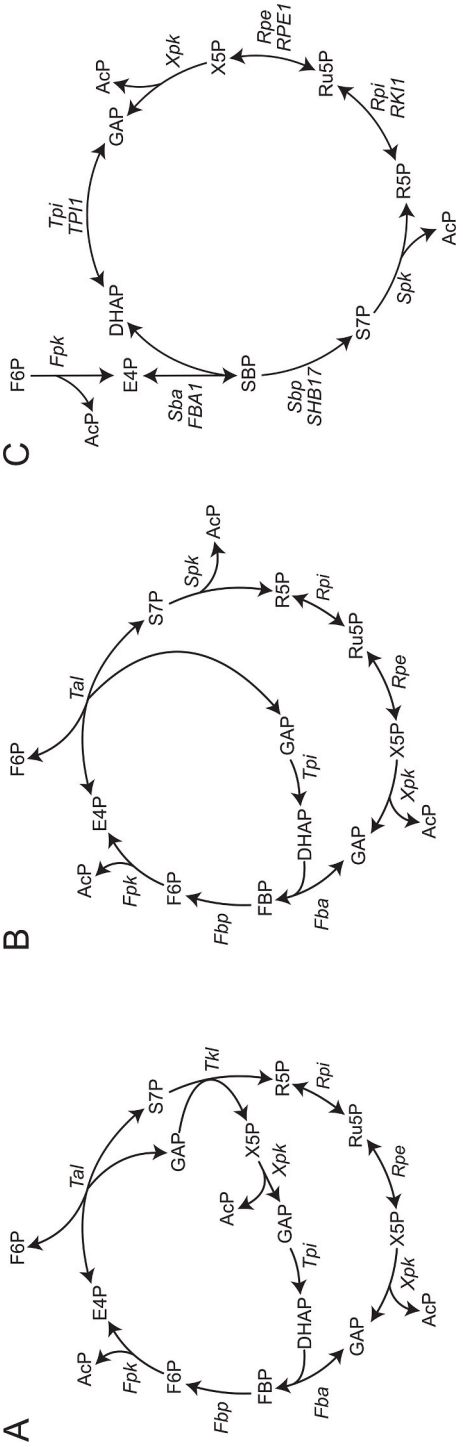


**Fig. 1.** Carbon-conserving pathways. **A)** The non-oxidative glycolysis (NOG) (Bogorad et al., 2013), **B)** the phosphoketolase shunt (Krüsemann et al., 2018) and **C)** the **G**lycolysis **AlT**ernative **H**igh **C**arbon **Y**ield **C**ycle (GATHCYC). The native *S. cerevisiae* genes are in included in C). The phosphoketolase reactions are all catalyzed by the *B. longum* phosphoketolase. Abbreviations: AcP, acetyl-phosphate; DHAP, dihydroxyacetone phosphate; E4P, erythrose-4-phosphate; F6P, fructose-6-phosphate; Fba, fructose-1,6-bisphosphate aldolase; FBP, fructose-1,6-bisphosphate; Fbp, fructose-1,6-bisphosphatase; Fpk, phosphoketolase (F6P activity); GAP, glyceraldehyde-3-phosphate; R5P, ribose-5-phosphate; Rpe, ribulose-5-phosphate 3-epimerase; Rpi, ribose-5-phosphate isomerase; Ru5P, ribulose-5-phosphate; S7P, sedoheptulose-7-phosphate; Sba, sedoheptulose-1,7-bisphosphate aldolase; SBP, sedoheptulose-1,7-bisphosphate; Sbp, sedoheptulose-1,7-bisphosphatase; Spk, phosphoketolase (S7P activity); Tal, transaldolase; Tkl, transketolase; Tpi, triose phosphate isomerase; X5P, xylulose-5-phosphate; Xpk, phosphoketolase (X5P activity).

reaction by Shb17, and both reactions are part of the riboneogenesis pathway in *S. cerevisiae* (Clasquin et al., 2011).

In this paper, we first show that the NOG configuration contains a kinetic bottleneck, which is resolved in the phosphoketolase shunt and the GATHCYC cycle. Secondly, we prove *in vitro* and *in vivo* activity of the GATHCYC pathway, using *S. cerevisiae* as the host. Finally, we show that this pathway increases the yield of the industrially relevant product 3-hydroxypropionic acid (3-HP) during growth on glucose.

## 2. Results

### 2.1. COPASI model simulations

Carbon-conserving pathways have the potential to increase product yields, but bottlenecks in the pathway could result in too low reaction rates and diminish, or even abolish, the benefit of a carbon-conserving pathway. In order to evaluate bottlenecks of the NOG pathway (Bogorad et al., 2013), a computational method based on the COPASI algorithm (Hoops et al., 2006) (http://copasi.org/) was employed using the reactions of the NOG pathway, including chemical species, enzyme concentrations and kinetic parameters of each reaction. The kinetic parameters were extracted from published data (Messiha et al., 2014; Smallbone et al., 2013; Teusink et al., 2000) and from data deposited on the Biomodels website (https://www.ebi.ac.uk/biomodels/BIOMD0000000064). The enzyme concentrations were set not to limit the reaction flux when the substrates are available.

The steady state simulation of NOG on fructose with a specific (Fig. S1) or generalist phosphoketolase (Fig. 2A) shows accumulation of intermediates, mostly S7P, that *in vivo* would normally block the use of the NOG pathway. A sensitivity analysis (Table S1) showed a strong correlation of S7P concentration and the equilibrium constants (Keq) of several enzymes: triose phosphate isomerase (Tpi), fructose 1,6-bisphosphate aldolase (Fba), ribulose-5-phosphate 3-epimerase (Rpe) and transketolase (Tkl). The equilibrium constants are parameters linked to the thermodynamics of the reaction and thus cannot be improved using enzyme engineering. Thus, these NOG configurations can be thermodynamically and kinetically limited. The equilibrium constants, of Fba and Tpi in particular, indicate that the availability of glyceraldehyde 3-phosphate (GAP) will be limited. Thus, the pairing of GAP with S7P for the reaction Tkl: GAP + S7P → X5P + R5P or transaldolase (Tal): GAP + S7P → F6P + E4P is limited. The depletion of GAP will create a bottleneck at the Tkl step and lead to S7P accumulation.

To overcome this disadvantage, a new S7P activity (Spk) was proposed to be introduced. In Fig. S2, different NOG configurations with Spk activities are presented. Interestingly, in the presence of all three Xpk, Fpk and Spk activities, there is no need of transketolase in the phosphoketolase shunt (Fig. 1B and Fig. S2D. Moreover, Andersen et al. (2019) also proposed the introduction of two new activities, Sba and Sbp, which forms the GATHCYC (Fig. 1C). This removes the need of Tal, which reduces the complexity of the pathway. The removal of Tal and Tkl is beneficial, as they catalyze reversible reactions, act on multiple substrates and require two substrates simultaneously for the reaction to occur. The kinetic steady-state simulations of the phosphoketolase shunt and the GATHCYC both reached a steady state with no intermediates accumulating (Fig. 2B–C), which indicates that the kinetic bottleneck of the NOG is resolved. The GATHCYC was chosen for further evaluation *in vitro* and *in vivo*, as the phosphoketolase shunt has already been evaluated (Krüsemann et al., 2018) and because of the lower complexity of the GATHCYC.

### 2.2. In vitro pathway evaluation

The GATHCYC functionality in yeast was evaluated by deleting competing pathways and measuring *in vitro* formation of AcP from F6P. To enable the GATHCYC in *S. cerevisiae*, the transketolase (*TKL1*, *TKL2*) and the transaldolase genes (*TAL1*, *NQM1*) were deleted, in combination

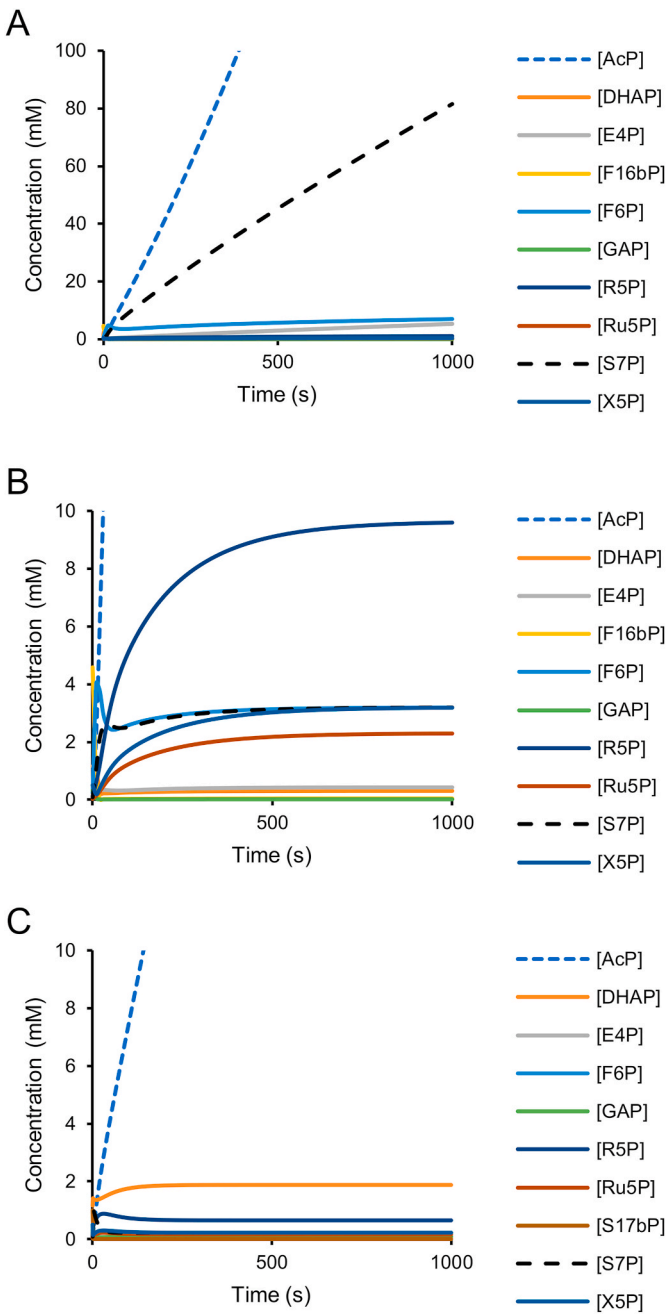


**Fig. 2.** Kinetic time course simulations of different carbon-conserving pathways on fructose, using the LSODA solver. **A)** NOG configuration with a generalist phosphoketolase results in continuous increase of the S7P concentration and does not reach steady state. **B)** The phosphoketolase shunt reaches a near steady state although with high plateau for R5P concentration. **C)** The GATHCYC configuration reaches steady state with low intermediate metabolite concentrations (<2 mM).

with overexpression of the native SBPase gene *SHB17* (Clasquin et al., 2011). Finally, *PHO13* was deleted to avoid formation of sedoheptulose (Xu et al., 2016), and *xfspk* from *B. longum* was expressed from an episomal plasmid. A pathway-negative strain (JH10) was constructed as a control, which has the GATHCYC cycle disrupted through deletion of *SHB17* (Fig. 3A). This strain will produce 3 times less AcP compared to the pathway-positive strain (JH9) if the pathway is functional. These two strains were evaluated in an *in vitro* phosphoketolase assay using crude cell free extracts (Bergman et al., 2016; Racker, 1962) (Fig. 3B), where the pathway-positive strain yielded a 2.7 times higher signal than

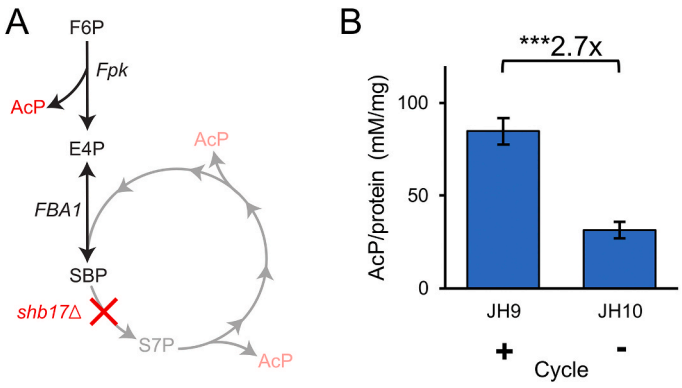


**Fig. 3.** GATHCYC pathway evaluation through an *in vitro* phosphoketolase assay on crude cell free extracts. **A)** Both strains have the required GATHCYC background and express *xfspk* from a high copy plasmid. The pathway-negative strain (JH10) is *shb17*Δ and cannot utilize the full cycle (faded). The pathway-positive strain (JH9) will utilize the full GATHCYC cycle through *SHB17* overexpression and is expected to produce 3 times more AcP than the pathway negative strain. **B)** Results of the phosphoketolase assay on crude cell free extracts. Strains were grown in biological triplicates and assayed in technical duplicates; error bars show the standard deviation. Asterisk (***) indicate a significant difference ($p < 0.001$, two-sided Student's t-test with unequal variance).

the control strain. The expected results align very well with the observed data, indicating that the pathway is functional.

### 2.3. *In vivo* pathway evaluation

*In vivo* activity was demonstrated by constructing a strain that was dependent on a functional GATHCYC cycle to survive, see Fig. 4A. Knockout of both transketolase genes and the glucose-6-phosphate dehydrogenase gene (*ZWF1*) has been reported to be lethal for *S. cerevisiae*, even when grown in rich media (Schaaff-Gerstenschläger et al., 1993). These deletions block the formation of R5P, needed for histidine and nucleotide biosynthesis (Deutscher et al., 2006; Krüsemann et al., 2018). Only strains with a functional GATHCYC cycle will be able to produce the R5P required for growth, similar to the experimental setup regarding the phosphoketolase shunt (Krüsemann et al., 2018).

The GATHCYC strain was further engineered by integrating 2 copies of *xfspk*, 1 copy of *pta* from *Clostridium kluyveri* and by deletion of *GPP1* to reduce the promiscuous breakdown of AcP to acetate (Bergman et al., 2016; Meadows et al., 2016). In this strain (JH25), *ZWF1* was successfully deleted (JH40) and the GATHCYC was shown to support growth when grown in minimal media (Fig. 4B). *ZWF1* deletion was not possible in the *shb17*Δ background (JH46). Therefore, *ZWF1* was instead downregulated when grown on glucose by exchanging the *ZWF1* promoter with the *GAL1* promoter (JH45) as a negative control. This creates a system where *ZWF1* is expressed in galactose conditions, but only at very low levels when glucose is present (Weinhandl et al., 2014). JH45 was constructed with galactose as a carbon source and *ZWF1* downregulation was shown to reduce the growth rate in this background when grown in minimal media with glucose (strain JH45 and JH46, Fig. 4B). *ZWF1* downregulation did not have a major effect in the GATHCYC background (strain JH44, Fig. 4B); however, its deletion resulted in a longer lag phase and lower growth rate, while still reaching the same biomass level (strain JH40, Fig. 4B). These results show that the cycle has sufficient activity *in vivo* to rescue the R5P deficiency in a *tkl1*Δ *tkl2*Δ *zwf1*Δ background. The combined results from the *in vitro* and *in vivo* experiment show that the GATHCYC pathway is functional and can now be extended to produce a proof-of-concept product to test the strain for improved yields.

### 2.4. 3-HP production in yeast

3-Hydroxypropionic acid (3-HP) was chosen as a proof-of-concept product for evaluation of the GATHCYC cycle as improved acetyl-CoA supply has previously been shown to increase 3-HP titers (Chen et al., 2014). 3-HP is produced from acetyl-CoA in two steps: conversion of acetyl-CoA to malonyl-CoA by acetyl-CoA carboxylase, which is further converted to 3-HP by a two-step NADPH dependent reduction by malonyl-CoA reductase (MCR). JH25 was further engineered by integrating the gene encoding a deregulated acetyl-CoA carboxylase (*ACC1***) (Shi et al., 2014) into the genome and expressing the MCR from *Chloroflexus aurantiacus* ($mcr_{ca}$) (Hügler et al., 2002) from a high-copy plasmid. The final strain (JH27) was evaluated in shake flasks containing minimal media over 5 days for 3-HP production, and compared to a control strain with the phosphoketolase pathway but lacking the GATHCYC cycle (JH34). The GATHCYC resulted in 31% higher 3-HP levels, with 375 mg/L and 286 mg/L for JH27 and JH34, respectively (Fig. 5A), and 62% higher when normalized to the biomass (Fig. 5B), showing a benefit of using the GATHCYC with the $mcr_{ca}$ expressed from a high copy plasmid.

3-HP production was also evaluated in a strain with more stable expression of $mcr_{ca}$ resulting from genomic integration to avoid possible effects from potential differences in the plasmid copy number between the cycle and control strain. One copy of the bifunctional $mcr_{ca}$ under the control of the enhanced *TDH3* promoter (Blazeck et al., 2012) increased the maximal growth rate in the GATHCYC strain from 0.13 to 0.19 $h^{-1}$ and control strain from 0.2 to 0.23 $h^{-1}$ compared to plasmid-based expression (Fig. S3). Furthermore, the GATHCYC increased the 3-HP titer by 63% when glucose was exhausted, with 89 mg/L and 54 mg/L for JH28 and JH37, respectively, showing a benefit of the GATHCYC during the glucose phase (Fig. S4). However, one copy of $mcr_{ca}$ yielded lower 3-HP titers for both strains and no improvement in 3-HP titers for the GATHCYC strain when the produced ethanol is consumed at the end of the ethanol phase: 121 and 133 mg/L 3-HP for JH28 and JH37, respectively at 72 h. These observations were verified by separating the native bifunctional $mcr_{ca}$ into two subdomains, provided by Li et al. (unpublished data), which increases the activity of the enzyme. The more efficient $mcr_{ca}$ showed an even higher benefit from of the GATHCYC during the glucose phase, with a 109% increase in 3-HP titer when glucose was exhausted (Fig. 6A). The split $mcr_{ca}$ resulted in overall higher 3-HP titers for both strains, but the GATHCYC showed no increase in final titers compared to the control after 96 h of cultivation (Fig. 6B).

## 3. Discussion

In this study, we evaluated the GATHCYC (Fig. 1C), a novel carbon-conserving cycle, proposed by Andersen et al. (2019) as a variant of the NOG, for cytosolic acetyl-CoA supply in *S. cerevisiae*. Obtaining a platform strain with higher yields for acetyl-CoA derived products is very attractive as it will reduce the amount of carbon wasted, which can make the process more profitable. Several cyclic pathways have been evaluated for carbon conservation (François et al., 2020), including NOG (Bogorad et al., 2013; Lin et al., 2018), EP-bifido (Wang et al., 2019) and glycoptimus (Lachaux et al., 2019). *In silico* analysis showed that the GATHCYC cycle circumvents the kinetic bottleneck of the NOG (Fig. 2), which suggests that it is more efficient. However, further *in vitro* and *in vivo* experiments are required to prove that this bottleneck is resolved. The GATHCYC cycle was enabled by the trifunctionality of the

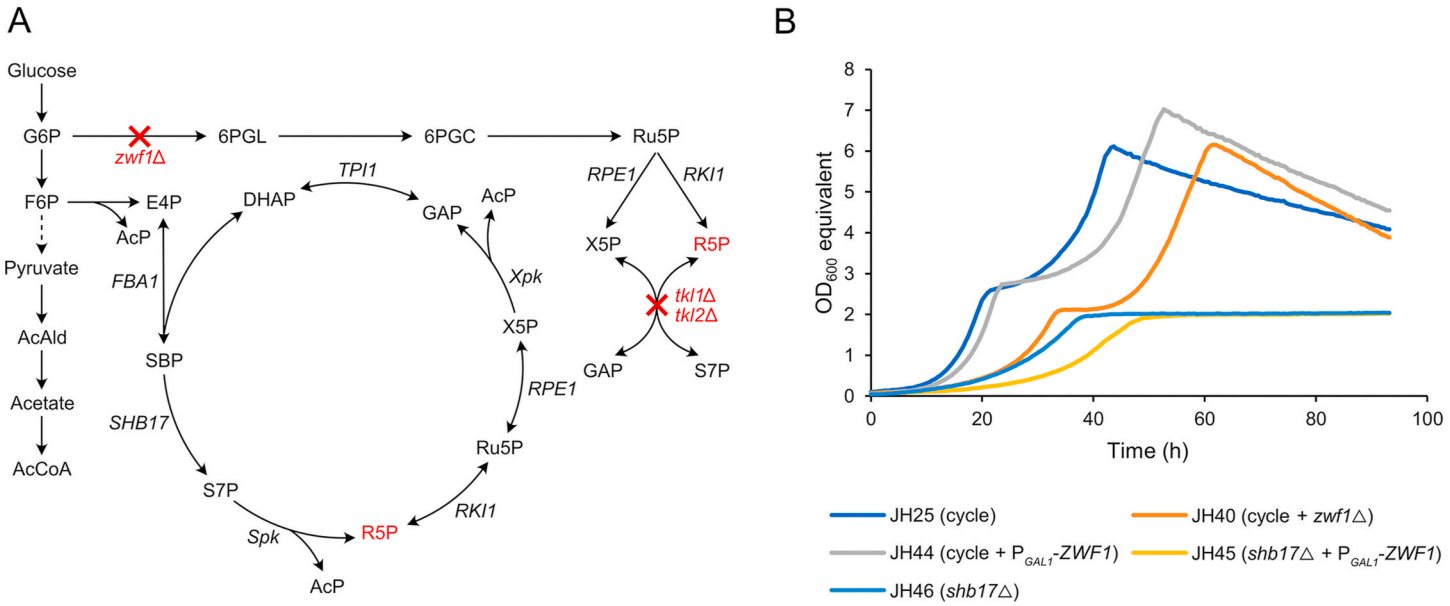


**Fig. 4.** Evaluation of the GATHCYC *in vivo*. **A)** The *tkl1*Δ *tkl2*Δ *zwf1*Δ background requires a functional GATHCYC cycle to produce R5P (marked in red) from glucose. **B)** Microtiter plate growth of GATHCYC strain (JH25), GATHCYC with *zwf1*Δ (JH40), GATHCYC with downregulated *ZWF1* (JH44), disrupted GATHCYC from *shb17*Δ (JH46) and disrupted GATHCYC with *ZWF1* downregulation (JH45). Strains were grown in 250 μL minimal media containing 2% glucose and 100 mg/L uracil, using biological and technical triplicates. JH45 was precultured in rich media with galactose as the carbon source. (For interpretation of the references to colour in this figure legend, the reader is referred to the Web version of this article.)

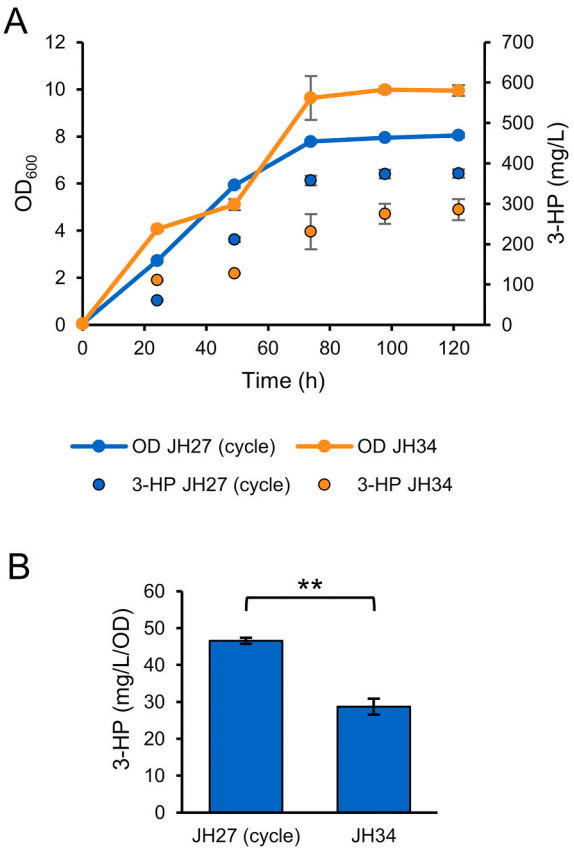


**Fig. 5.** 3-HP production comparison between GATHCYC (JH27) and phosphoketolase only (JH34) precursor supply pathway, with the $mcr_{ca}$ expressed from a high copy plasmid. **A)** Optical density ($OD_{600}$) and extracellular 3-HP concentration during 5 days of cultivation and **B)** 3-HP concentration normalized to $OD_{600}$ after 5 days of cultivation. Strains were grown in minimal media containing 2% glucose, using biological triplicates; error bars show the standard deviation. Statistical analysis was performed with two-sided Student's t-test with unequal variance (**p < 0.01).

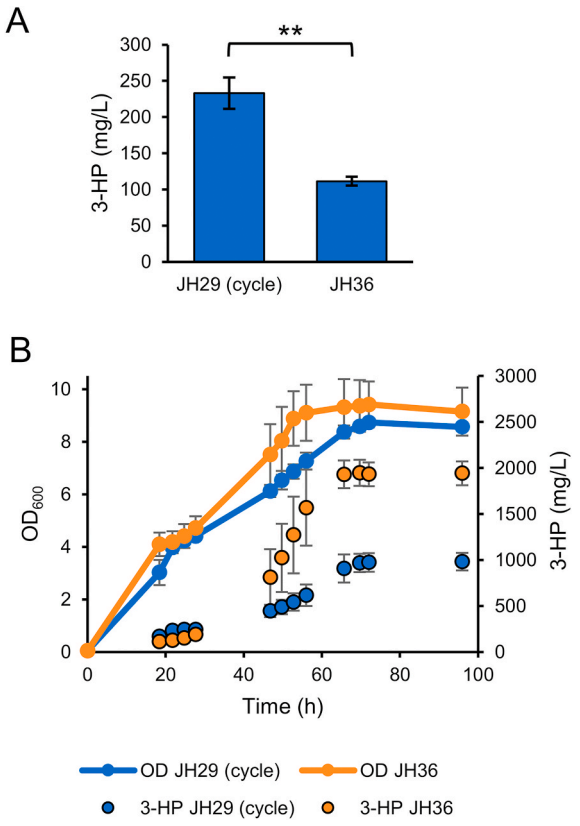


**Fig. 6.** 3-HP production comparison between GATHCYC (JH29) and phosphoketolase only (JH36) precursor supply pathway, with the split $mcr_{ca}$ expressed from the genome. **A)** 3-HP titers at glucose exhaustion and **B)** optical density ($OD_{600}$) and extracellular 3-HP concentrations during 4 d of cultivation. Strains were grown in 50 mL minimal media containing 2% glucose and 100 mg/L uracil, using biological triplicates; error bars show the standard deviation. Statistical analysis was performed with two-sided Student's t-test with unequal variance (**p < 0.01).

phosphoketolase from *B. longum*, which after carbon rearrangement reactions can produce 3 mol of AcP from 1 mol of F6P. *In vitro* activity of the cycle was demonstrated by constructing a control strain with *SHB17* deletion to disrupt the cycle after the first phosphoketolase reaction, and the 3:1 ratio of formed AcP from F6P confirmed the functionality of the cycle (Fig. 3).

*E. coli* also possesses all the enzymes necessary for the GATHCYC, except the phosphoketolase. The Sba reaction is performed by the native FbaA (Nakahigashi et al., 2009; Woolston et al., 2018) and SBPase activity has been found for the native GlpX (Woolston et al., 2018). However, the major substrate for GlpX is FBP (Brown et al., 2009), while the *S. cerevisiae* Shb17 is more specific to SBP (Clasquin et al., 2011), making Shb17 a better choice for the GATHCYC.

GATHCYC yeast strains without a phosphoketolase did not grow in minimal media. A high flux through the phosphoketolase is important to provide E4P to the shikimate pathway (Liu et al., 2019), as the aromatic amino acid (AAA) auxotrophy from the *tkl1*Δ *tkl2*Δ background (Schaaff-Gerstenschläger et al., 1993) is rescued by expression of *xfspk* from a 2μ plasmid or via genomic integration. Furthermore, genomic integration required 2 copies of *xfspk* to abolish the growth defect caused by lack of AAA, as addition of 1 more copy decreased lag time from 20 to 2.5 h, and increased maximal specific growth rate from 0.13 to 0.19 $h^{-1}$ (strain JH18 and JH28, Figs. S3 and S5). This shows that Xfspk activity is limiting and coupled to growth, and could thus be improved by adaptive laboratory evolution. A previous study showed an 80% increase in catalytic efficiency on F6P of the phosphoketolase from *Bifidobacterium adolescentis* when evolved in a host with defective phosphofructokinase (Dele-Osibanjo et al., 2019).

We were able to show that the GATHCYC has sufficient activity *in vivo* to support growth in *tkl1*Δ *tkl2*Δ *zwf1*Δ, where all the R5P has to be produced from the GATHCYC (Fig. 4). In a strain with disrupted GATHCYC through deletion of *SHB17*, it was impossible to delete *ZWF1* as well, and it showed reduced growth when *ZWF1* was downregulated with the *GAL1* promoter on glucose (strain JH45 and JH46, Fig. 4B). Downregulation of *ZWF1* in the cycle strain did not reduce strain performance; however, its deletion resulted in slightly reduced growth (strain JH25, JH40 and JH44, Fig. 4B), indicating leakage of the *GAL1* promoter at glucose conditions. This could explain why *ZWF1* downregulation still enables growth of the GATHCYC disrupted strain even though its deletion seemed to be lethal.

The GATHCYC makes an effective route, in terms of carbon saving, towards acetyl-CoA. In this study, we did however not restrict the carbon flux through the GATHCYC alone due to the observed growth defect of strains relying on NOG (Lin et al., 2018), which also showed no growth-coupled production of acetate and a lack of reducing power. The GATHCYC suffers the same drawbacks as NOG (François et al., 2020), which means that it is beneficial for producing acetate, as acetate production generates 2 ATP/glucose and requires no redox factor, but not for products that are more reduced than acetate. This led us not to disrupt *ZWF1*, *PFK1-2*, *TDH1-3* or *PGK1* for 3-HP production. A promising configuration for obtaining a high yield of acetyl-CoA derived products is by combining a carbon-conserving pathway together with a route to acetyl-CoA that produces ATP (Dele-Osibanjo et al., 2019;

Meadows et al., 2016; van Rossum et al., 2016). This could for instance be achieved by using the GATHCYC and the acetylating acetaldehyde dehydrogenase pathway for acetyl-CoA supply, where most of the NADPH is generated from the oxidative pentose phosphate pathway.

A combination of NOG and the native pathway in *E. coli* has been evaluated for acetone production, which improved yields from 0.38 to 0.47 mol acetone/mol glucose (Yang et al., 2016). However, it was unclear if the yield improvement was caused by the phosphoketolase alone or from the NOG configuration. The phosphoketolase pathway should provide 1.5 mol of acetyl-CoA without carbon loss from glucose (Suzuki et al., 2010), whereas the NOG configuration should provide 3 mol acetyl-CoA. In this study, we separated the yield increase of the GATHCYC from the phosphoketolase pathway alone by constructing a control strain (JH34) with the same background as the GATHCYC strain (JH27), except the modifications required for the GATHCYC (*tkl1*Δ, *tkl2*Δ, *tal1*Δ, *nqm1*Δ and *SHB17* overexpression). The 31% increase in 3-HP titers and 63% increase when normalized to biomass (Fig. 5) indicated that the cycle increased the acetyl-CoA supply during plasmid-based expression of $mcr_{ca}$.

3-HP production from strains with genomic integration of the $mcr_{ca}$ was also evaluated to rule out possible effects from differences in copy number of the high copy plasmid. Integration of one copy of $mcr_{ca}$ improved growth rates and final $OD_{600}$ for both strains compared to plasmid-based expression, but only improved the 3-HP titer during the glucose phase and mid ethanol phase (Figs. S3, S4 and S7). The low 3-HP levels from both strains suggested a possible bottleneck in the flux to 3-HP from malonyl-CoA, which could limit the benefit of increased precursor supply. Therefore, the more efficient split $mcr_{ca}$ was utilized to achieve higher and stable 3-HP production. The split $mcr_{ca}$ resulted in similar growth rates compared to native $mcr_{ca}$ (Figs. S3 and S8), but more than double 3-HP titers compared to the control when glucose was consumed (Fig. 6A), verifying the increased precursor supply of acetyl-CoA by the cycle during the glucose phase. The precursor supply during the ethanol phase was not improved by the GATHCYC, with no final increase in 3-HP titers. This contradicts the plasmid-based results, but other factors, such as strain background, might have influenced the copy number of the plasmid with $mcr_{ca}$. This makes the results from the integrated $mcr_{ca}$ more reliable. The GATHCYC relies on efficient flux through the phosphoketolase, and a previous study showed that the Xfpk/Pta route only improved precursor supply for free fatty acids during the glucose phase (Bergman et al., 2019b).

The maximum acetate levels of the 3-HP producing strains ranged between 2 and 3 g/L (Figs. S6, S7 and S9). Accumulation of acetate is problematic as it acidifies the cytoplasm, and the cell is required to spend energy on pumping out acetate ions to maintain intracellular pH homeostasis (Ramos et al., 2016). Elevated amounts of acetate have been shown to be the result of phosphoketolase expression, where acetate levels increased from 0.55 g/L to 1.1 g/L (Bergman et al., 2019a), which is usually resolved by *GPP1* deletion (Bergman et al., 2016; Meadows et al., 2016). The high acetate levels in the strains in this study might be caused by a limitation in the flux from acetyl-CoA to malonyl-CoA, allowing AcP produced by the phosphoketolase to be hydrolyzed to acetate instead of being converted to acetyl-CoA by Pta. Another explanation could be an increased NADPH demand (Ferreira et al., 2004) during 3-HP production, as acetate production generates NADPH and high acetate levels have been observed in 3-HP producing strains before (Kildegaard et al., 2016). The high level of acetate for JH29 during the ethanol phase compared to JH36 could possibly explain the lower performance in 3-HP production of JH29 during the ethanol phase (Fig. 6B and Fig. S9).

Glycerol is produced to oxidize excess NADH resulting from biomass formation during fermentative growth, which is important for maintaining the redox balance (Dijken and Scheffers, 1986). The produced glycerol was readily consumed by the control strains, which was not the case for the GATHCYC strains (Figs. S6, S7 and S9). CEN. PK strains do not grow on glycerol as a sole carbon source (Swinnen et al., 2013), but should be able to metabolize glycerol when ethanol is present in the media (van Dijken et al., 2000). The inability of the GATHCYC strains to consume all the produced glycerol could be due to a redox imbalance, which could limit the performance of the GATHCYC strain. This redox imbalance is assumed to be indirectly caused by the disruption of the non-oxidative pentose phosphate pathway. Replacement of the non-oxidative pentose phosphate pathway with the GATHCYC pathway supports growth on the nonfermentable carbon sources ethanol and acetate but leaves 0.6–0.9 g/L glycerol in the media. Thorough characterization of these strains in bioreactors is required to investigate this possible redox imbalance and uncover the reasons why glycerol is not fully consumed, with the end goal to further improve yields and strain performance.

There are still optimizations needed to fully utilize the GATHCYC. Currently, GATHCYC strains have a longer glucose phase (Fig. S9), show a lower maximal growth rate (Figs. S3 and S8) and reach a lower final $OD_{600}$ (Figs. 5 and 6 and S4) compared to the control strain with only the phosphoketolase pathway. Adding a second copy of the phosphoketolase gene greatly improved strain performance (strain JH18 and JH28, Figs. S3 and S5), but still not to the level of the control. Phosphoketolase activity could still be limiting and balancing between the X5P, F6P and S7P activities might be necessary to increase strain performance further. Replacement of the non-oxidative pentose phosphate pathway with this artificial cycle could require additional strain engineering to reduce the growth defect appearing from this dramatic change in the central carbon metabolism. Extensive strain characterization will aid in uncovering the genomic modifications needed to improve strain performance of the GATHCYC strains.

This study shows that the GATHCYC alone, without optimization of the native pathway to acetyl-CoA, results in a doubling of 3-HP titers at glucose exhaustion. Higher 3-HP titers could potentially be reached by increasing the copy number of the *mcr* gene, overexpression of PDH bypass genes, co-factor balancing and fed-batch fermentation as shown before (Kildegaard et al., 2016), combined with the GATHCYC as a carbon-conserving route to acetyl-CoA. van Rossum et al. (2016) showed that balancing the fluxes to acetyl-CoA between the carbon-conserving pathway NOG and pathways that generate co-factors and energy is expected to produce the highest yield of acetyl-CoA derived products. GATHCYC has the same acetyl-CoA yield and similar carbon rearrangement reactions as NOG and should therefore be compatible with this approach and be able to replace NOG as the carbon-conserving pathway. However, this needs to be experimentally verified.

In conclusion, this study demonstrates a novel functional carbon-conserving cycle for acetyl-CoA supply in *S. cerevisiae*. The cycle was shown to be active *in vitro*, supporting growth in a *zwf1*Δ strain and increasing 3-HP titers by 109% after the glucose phase. With more optimization, the GATHCYC will be a value addition to a platform strain with increased yields of acetyl-CoA derived industrial products.

## 4. Materials and methods

### 4.1. COPASI model simulations

Kinetic time course simulations of the carbon-conserving pathways were performed in COPASI, using the LSODA solver. Table S2 shows the kinetic parameters and initial concentrations of the species in the model. Different preferences of the phosphoketolase (XPK, FPK, SPK) were simulated by setting Vmax for each reaction to 0 mmol/(l*s) if no reaction and to 0.6 mmol/(l*s) if the flux is needed. Fluxes were blocked when necessary by changing respective enzyme concentration from 1 to 0 mmol/L.

### 4.2. Cultivation media

All chemicals were purchased from Sigma-Aldrich/Merck, unless

**Table 1**
*S. cerevisiae* strains used in this study.

| Strain | Genotype | Notes | Origin |
|---|---|---|---|
| IMX581 | *MATa ura3-52 can1Δ::cas9-natNT2 TRP1 LEU2 HIS3* | Cas9 expressing | Mans et al. (2015) |
| JH9 | IMX581 *tkl1/2Δ tal1Δ nqm1Δ pho13Δ* $P_{SHB17}$Δ::$P_{TDH3}$ pBS01A-*xfspk* | Pathway **positive,** phosphoketolase assay | This study |
| JH10 | IMX581 *tkl1/2Δ tal1Δ nqm1Δ pho13Δ shb17Δ* pBS01A-*xfspk* | Pathway **negative,** phosphoketolase assay | This study |
| JH18 | IMX581 *tkl1/2Δ tal1Δ nqm1Δ pho13Δ* $P_{SHB17}$Δ::$P_{TDH3}$ *XII-1*::$P_{TEF1}$-*xfspk*-$T_{ADH1}$ | Pathway **positive,** 1 copy xfspk | This study |
| JH19 | IMX581 *tkl1/2Δ tal1Δ nqm1Δ pho13Δ shb17Δ* *XII-1*::$P_{TEF1}$-*xfspk*-$T_{ADH1}$ | Pathway **negative,** 1 copy xfspk | This study |
| JH25 | IMX581 *tkl1/2Δ tal1Δ nqm1Δ pho13Δ* $P_{SHB17}$Δ::$P_{TDH3}$ *XII-1*::$P_{TEF1}$-*xfspk*-$T_{ADH1}$ *XI-1*::$P_{eTDH3}$-*xfspk*-$T_{CYC1}$ *X-2*::$P_{eTEF1}$-*pta*-$T_{CYC1}$ *gpp1Δ* | Pathway **positive** | This study |
| JH27 | IMX581 *tkl1/2Δ tal1Δ nqm1Δ pho13Δ* $P_{SHB17}$Δ::$P_{TDH3}$ *XII-1*::$P_{TEF1}$-*xfspk*-$T_{ADH1}$ *XI-1*::$P_{eTDH3}$-*xfspk*-$T_{CYC1}$ *X-2*::$P_{eTEF1}$-*pta*-$T_{CYC1}$ *gpp1Δ X-4*::$P_{HXT7}$-*ACC1***-$T_{CYC1}$ pBS01A-*mcr* | Pathway **positive,** 3-HP production | This study |
| JH28 | IMX581 *tkl1/2Δ tal1Δ nqm1Δ pho13Δ* $P_{SHB17}$Δ::$P_{TDH3}$ *XII-1*::$P_{TEF1}$-*xfspk*-$T_{ADH1}$ *XI-1*::$P_{eTDH3}$-*xfspk*-$T_{CYC1}$ *X-2*::$P_{eTEF1}$-*pta*-$T_{CYC1}$ *gpp1Δ X-4*::$P_{HXT7}$-*ACC1***-$T_{CYC1}$ *XI-3*::$P_{eTDH3}$-*mcr*-$T_{CYC1}$ | Pathway **positive,** 3-HP production | This study |
| JH29 | IMX581 *tkl1/2Δ tal1Δ nqm1Δ pho13Δ* $P_{SHB17}$Δ::$P_{TDH3}$ *XII-1*::$P_{TEF1}$-*xfspk*-$T_{ADH1}$ *XI-1*::$P_{eTDH3}$-*xfspk*-$T_{CYC1}$ *X-2*::$P_{eTEF1}$-*pta*-$T_{CYC1}$ *gpp1Δ X-4*::$P_{HXT7}$-*ACC1***-$T_{CYC1}$ *XI-3*::$P_{HXT7}$-*mcrC*-$T_{TEF2}$ + $P_{TEF1}$-*mcrN*-$T_{FBA1}$ | Pathway **positive,** 3-HP production, | This study |
| JH34 | IMX581 *XII-1*::$P_{TEF1}$-*xfspk*-$T_{ADH1}$ *XI-1*::$P_{eTDH3}$-*xfspk*-$T_{CYC1}$ *X-2*::$P_{eTEF1}$-*pta*-$T_{CYC1}$ *gpp1Δ X-4*::$P_{HXT7}$-*ACC1***-$T_{CYC1}$ pBS01A-*mcr* | Control, 3-HP production | This study |
| JH36 | IMX581 *XII-1*::$P_{TEF1}$-*xfspk*-$T_{ADH1}$ *XI-1*::$P_{eTDH3}$-*xfspk*-$T_{CYC1}$ *X-2*::$P_{eTEF1}$-*pta*-$T_{CYC1}$ *gpp1Δ X-4*::$P_{HXT7}$-*ACC1***-$T_{CYC1}$ *XI-3*::$P_{HXT7}$-*mcrC*-$T_{TEF2}$ + $P_{TEF1}$-*mcrN*-$T_{FBA1}$ | Control, 3-HP production | This study |
| JH37 | IMX581 *XII-1*::$P_{TEF1}$-*xfspk*-$T_{ADH1}$ *XI-1*::$P_{eTDH3}$-*xfspk*-$T_{CYC1}$ *X-2*::$P_{eTEF1}$-*pta*-$T_{CYC1}$ *gpp1Δ X-4*::$P_{HXT7}$-*ACC1***-$T_{CYC1}$ *XI-3*::$P_{eTDH3}$-*mcr*-$T_{CYC1}$ | Control, 3-HP production | This study |
| JH40 | IMX581 *tkl1/2Δ tal1Δ nqm1Δ pho13Δ* $P_{SHB17}$Δ::$P_{TDH3}$ *XII-1*::$P_{TEF1}$-*xfspk*-$T_{ADH1}$ *XI-1*::$P_{eTDH3}$-*xfspk*-$T_{CYC1}$ *X-2*::$P_{eTEF1}$-*pta*-$T_{CYC1}$ *gpp1Δ zwf1Δ* | Pathway **positive,** *ZWF1* disrupted | This study |
| JH44 | IMX581 *tkl1/2Δ tal1Δ nqm1Δ pho13Δ* $P_{SHB17}$Δ::$P_{TDH3}$ *XII-1*::$P_{TEF1}$-*xfspk*-$T_{ADH1}$ *XI-1*::$P_{eTDH3}$-*xfspk*-$T_{CYC1}$ *X-2*::$P_{eTEF1}$-*pta*-$T_{CYC1}$ *gpp1Δ* $P_{ZWF1}$Δ::$P_{GAL1}$ | Pathway **positive,** *ZWF1* downregulated on glucose | This study |
| JH45 | IMX581 *tkl1/2Δ tal1Δ nqm1Δ pho13Δ* *XII-1*::$P_{TEF1}$-*xfspk*-$T_{ADH1}$ *XI-1*::$P_{eTDH3}$-*xfspk*-$T_{CYC1}$ *X-2*::$P_{eTEF1}$-*pta*-$T_{CYC1}$ *gpp1Δ shb17Δ* $P_{ZWF1}$Δ::$P_{GAL1}$ | Pathway **negative,** *ZWF1* downregulated on glucose | This study |
| JH46 | IMX581 *tkl1/2Δ tal1Δ nqm1Δ pho13Δ* *XII-1*::$P_{TEF1}$-*xfspk*-$T_{ADH1}$ *XI-1*::$P_{eTDH3}$-*xfspk*-$T_{CYC1}$ *X-2*::$P_{eTEF1}$-*pta*-$T_{CYC1}$ *gpp1Δ shb17Δ* | Pathway **negative** | This study |

otherwise specified. The growth medium for yeast strain construction was yeast-peptone-dextrose (YPD), containing 10 g/L yeast extract, 20 g/L peptone from meat and 20 g/L glucose. *E. coli* DH5α was used for plasmid construction and grown in lysogeny broth (LB), composed of 5 g/L yeast extract, 10 g/L peptone from casein and 10 g/L NaCl. Agar-agar was added at 20 g/L and 16 g/L to make YPD and LB plates, respectively.

*E. coli* transformants were selected on LB plates supplemented with 100 μg/mL ampicillin. Selection of yeast transformants was performed on synthetic complete dropout (SD) plates without uracil, which contained 6.9 g/L yeast nitrogen base (YNB) without amino acids (Formedium), 0.77 g/L complete supplement mix (CSM) without uracil (Formedium), 20 g/L glucose and 20 g/L agar-agar. 5-Fluoroorotic acid (5-FOA) plates (containing 6.9 g/L YNB without amino acids, 0.77 g/L CSM without uracil, 50 mg/L uracil, 1 g/L 5-FOA (Formedium), 20 g/L glucose and 20 g/L agar-agar) was used to remove the *URA3* marker.

Cultivations prior phosphoketolase assay and 3-HP measurements were performed in minimal medium, which contained 7.5 g/L $(NH_4)_2SO_4$, 14.4 g/L $KH_2PO_4$, 0.5 g/L $MgSO_4{\cdot}7H_2O$, 20 g/L glucose, 1 mL/L vitamin solution, 2 mL/L trace metal solution and pH set to 6.5 with KOH. The vitamin solution and trace metal solution were prepared as previously described (Verduyn et al., 1992). Glucose was added at concentration of 20 g/L. Yeast was precultured in 14 mL cultivated tubes and main cultures consisted of 20 mL minimal medium in 100 mL unbaffled shake flasks incubated at 30 °C with 200 rpm orbital shaking. 50 mL yeast cultures were cultivated in 250 mL unbaffled shake flasks. Cell density was measured through optical density at 600 nm ($OD_{600}$).

### 4.3. Yeast strain and plasmid construction

The strains used in this study are shown in Table 1. *S. cerevisiae* IMX581, derived from *S. cerevisiae* CEN. PK113-5D (Entian and Kötter, 2007), was used as the parental strain. Genomic modifications of *S. cerevisiae* IMX581 was performed by introducing a guide-RNA (gRNA) expressing plasmid according to workflow by Mans et al. (2015).

*E. coli* transformations were performed according to Inoue et al. (1990). Table S3 shows all the plasmids used in this study. The plasmid pBS01A-*xfspk* contains the promiscuous phosphoketolase gene from *Bifidobacterium longum* NCC2705.

All kits, enzymes and buffers were ordered from Thermo Fisher Scientific, unless otherwise specified. The gRNA sequences were designed with the online tool Benchling (https://benchling.com) and are listed in Table S4. PCR was performed with Phusion High-Fidelity DNA Polymerase and products purified using either the GeneJET Gel Extraction or PCR Purification Kit. Primers were ordered from Eurofins Genomics.

Single and double genomic modifications were performed by cloning the gRNAs into pMEL10 and pROS10, respectively, using Gibson assembly (NEB). The assembled plasmid was used to transform *E. coli*, extracted with the GeneJET Plasmid Miniprep Kit and verified by Sanger sequencing (Eurofins Genomics). Transformation of yeast was performed with the lithium acetate/PEG method (Gietz, 2014).

Repair fragments for gene deletions were ordered as two complementary 120 bp oligos (60 bp upstream and 60 bp downstream of the gene) and annealed before transformation. Sequences for repair fragment oligos are found in Table S5. Fusion PCR (Zhou et al., 2012) was used to construct repair fragments for promoter replacement and the *XII-1*:$P_{TEF1}$-*xfspk* cassette integration. The remaining genomic

integrations were performed with the EasyClone-MarkerFree kit (Jessop-Fabre et al., 2016). All primers used to generate the plasmid and repair constructs are found in Table S6. Transformants were verified through colony PCR and Sanger sequencing of the PCR product. Sequences of diagnostic primers are found in Table S7. The *URA3* marker was recycled from successful transformants by plating on 5-FOA plates, and loss of plasmid confirmed by plating single colonies on both YPD and SD -ura plates. Clones that did not grow on SD -ura plates were cultivated in YPD overnight and cryopreserved at -80 °C in 15% sterile glycerol, using a CoolCell container to maintain viability during freezing.

The gene coding for the phosphoketolase from *Bifidobacterium longum* NCC2705 (GenBank: AAN24771.1) was codon optimized for *S. cerevisiae* by Genscript (Table S8). The codon optimized *xfspk* was cloned into pBS01A (Hu et al., 2017) by restriction cloning with BcuI and NotI, placing it downstream of the *TEF1* promoter.

### 4.4. Yeast phosphoketolase assay

The pathway was tested using purified crude cell free extracts. Briefly, single colonies of JH9 and JH10 were precultured for 3 d in 2 mL minimal media, using biological triplicates. The precultures were added to shake flasks containing 20 mL media at a starting $OD_{600}$ of 0.1 and cultivated until an $OD_{600}$ of 1. The cells were washed once with 10 mL MQ water and once with 10 mL protein extraction buffer (PEB), containing 50 mM potassium phosphate buffer, 1 mM dithiothreitol, 2 mM $MgSO_4$ and set to pH = 7.5. The cells were resuspended in 0.4 mL PEB and snap frozen in liquid $N_2$ after removal of the supernatant. The cell pellet was stored at -80 °C until lysis.

Cells were thawed on ice prior lysis, resuspended in 0.4 mL PEB and transferred to a 2 mL screw-cap tube containing 500 mg 425–600 μm glass beads (Sigma G-8772). Halt protease inhibitor cocktail (Thermo Fisher Scientific) was added to a final concentration of 1X. The cells were homogenized with a Precellys Evolution homogenizer, using 4 cycles of 6800 rpm for 20 s, and kept on ice for 5 min between the cycles. The homogenate was transferred to an Eppendorf tube and cell debris spun down at 20 000 g for 10 min at 0 °C. The supernatant was transferred to a fresh tube and stored on ice. Harvesting and lysis procedures were performed on ice with cold solutions. The lysis and assay were performed on the same day.

The protein concentration of the crude cell free extracts was determined in duplicates with a *DC* protein assay kit (Bio-Rad), using premade BSA standards (Thermo Fisher Scientific). The samples were diluted to the same protein concentration with PEB. Production of acetyl phosphate was evaluated with the ferric acetyl hydroxamate method (Lipmann and Tuttle, 1945; Racker, 1962), according to a protocol modified from Bergman et al. (2016). Briefly, the assay was performed in a 96-well microplate, using a reaction volume of 75 μL consisting of 50 mM potassium phosphate buffer (pH 7.5), 1 mM $MgSO_4$, 8 mM iodoacetate, 23 mM NaF, 90 mM F6P and 130 μg crude cell free extract. Reactions with lithium acetyl phosphate standards (0–16 mM) were performed in the same reaction buffer, but without F6P and crude cell free extract. The reaction was started by the addition of the crude cell free extract, and the microplate was incubated at room temperature for 2 h. The reaction was stopped, and the product converted to ferric acetyl hydroxamate, using the same procedure as described in Bergman et al. (2016), with the addition that the protein precipitate was removed by centrifuging the plate for 5 min at 2300 g. The supernatant was transferred to an empty plate and absorbance measured at 505 nm with the microplate reader FLUOstar® Omega (BMG Labtech GmbH).

### 4.5. 3-HP production

Single colonies of 3-HP producing strains were precultured in 2 mL minimal medium for 2 d. The precultures were used to inoculate 20 mL minimal medium at $OD_{600}$ = 0.05 and cultivated for up to 5 d. Samples for high-performance liquid chromatography (HPLC) were centrifuged at 12.000 g for 10 min (+4 °C) and extracellular concentrations of 3-HP, glucose, ethanol, acetate and glycerol were determined as previously described (Chen et al., 2014).

### 4.6. Growth profiler

Microtiter plate growth was performed in Growth Profiler 960 (Enzyscreen). Precultures were grown for 3 d in 2 mL minimal media supplemented with 100 mg/L uracil and used to inoculate 250 μL media at $OD_{600}$ = 0.05 in biological and technical triplicates, using a 96-well plate (Enzyscreen CR1496d). JH45 was precultured in rich media with galactose as a carbon source (20 g/L), washed with MQ-water and minimal media and resuspended in minimal media before inoculation of the microplate.

## Authors' contributions

J.H., A.G., J.N and V.S designed the research; J.H. performed the research; J.H. analyzed the data; A.G. performed the modelling; J.H. wrote the paper. All authors read and approved the final manuscript.

## Funding

The Novo Nordisk Foundation (grant no. NNF10CC1016517), Denmark.

The Chalmers Energy Area of Advance, Sweden.

The Swedish Energy Agency (grant no. P43548-1), Sweden.

Total S.A, France.

## Availability of data and materials

The model files for the COPASI models can be shared upon request.

## Consent for publication

Not applicable.

## Ethics approval and consent to participate

Not applicable.

## Declaration of competing interest

A.G. is an employee of TOTAL S.A. The patent WO/2019/166647 was filed on some aspects of this work.

## Acknowledgements

The authors would like to thank Xiaowei Li for providing the *mcr* genes, Quanli Liu for the pQC plasmids and Anastasia Krivoruchko for the pBS01A plasmid. The authors would also like to thank Olivier Vidalin (TOTAL S.A.) for project coordination.

## Appendix A. Supplementary data

Supplementary data to this article can be found online at https://doi.org/10.1016/j.ymben.2020.09.003.

## References

Andersen, J.L., Flamm, C., Merkle, D., Stadler, P.F., 2019. Chemical transformation motifs—modelling pathways as integer hyperflows. IEEE ACM Trans. Comput. Biol. Bioinf 16, 510–523. https://doi.org/10.1109/TCBB.2017.2781724.

Beck, Z.Q., Eliot, A.C., Peres, C.M., Vaviline, D. V, 2015. Utilization of phosphoketolase in the production of mevalonate, isoprenoid precursors, and isoprene. US Pat. 8,993,305.

Bergman, A., Hellgren, J., Moritz, T., Siewers, V., Nielsen, J., Chen, Y., 2019a. Heterologous phosphoketolase expression redirects flux towards acetate, perturbs sugar phosphate pools and increases respiratory demand in *Saccharomyces cerevisiae*. Microb. Cell Factories 18, 25. https://doi.org/10.1186/s12934-019-1072-6.

Bergman, A., Siewers, V., Nielsen, J., Chen, Y., 2016. Functional expression and evaluation of heterologous phosphoketolases in *Saccharomyces cerevisiae*. Amb. Express 6, 115. https://doi.org/10.1186/s13568-016-0290-0.

Bergman, A., Vitay, D., Hellgren, J., Chen, Y., Nielsen, J., Siewers, V., 2019b. Effects of overexpression of *STB5* in *Saccharomyces cerevisiae* on fatty acid biosynthesis, physiology and transcriptome. FEMS Yeast Res. 19, 27. https://doi.org/10.1093/femsyr/foz027.

Blazeck, J., Garg, R., Reed, B., Alper, H.S., 2012. Controlling promoter strength and regulation in *Saccharomyces cerevisiae* using synthetic hybrid promoters. Biotechnol. Bioeng. 109, 2884–2895. https://doi.org/10.1002/bit.24552.

Bogorad, I.W., Lin, T.-S., Liao, J.C., 2013. Synthetic non-oxidative glycolysis enables complete carbon conservation. Nature 502, 693–697. https://doi.org/10.1038/nature12575.

Brown, G., Singer, A., Lunin, V.V., Proudfoot, M., Skarina, T., Flick, R., Kochinyan, S., Sanishvili, R., Joachimiak, A., Edwards, A.M., Savchenko, A., Yakunin, A.F., 2009. Structural and biochemical characterization of the type II fructose-1,6-bisphosphatase GlpX from *Escherichia coli*. J. Biol. Chem. 284, 3784–3792. https://doi.org/10.1074/jbc.M808186200.

Chen, Y., Bao, J., Kim, I.-K., Siewers, V., Nielsen, J., 2014. Coupled incremental precursor and co-factor supply improves 3-hydroxypropionic acid production in Saccharomyces cerevisiae. Metab. Eng. 22, 104–109. https://doi.org/10.1016/j.ymben.2014.01.005.

Clasquin, M.F., Melamud, E., Singer, A., Gooding, J.R., Xu, X., Dong, A., Cui, H., Campagna, S.R., Savchenko, A., Yakunin, A.F., Rabinowitz, J.D., Caudy, A.A., 2011. Riboneogenesis in yeast. Cell 145, 969–980. https://doi.org/10.1016/j.cell.2011.05.022.

De Deken, R.H., 1966. The Crabtree effect: a regulatory system in yeast. J. Gen. Microbiol. 44, 149–156. https://doi.org/10.1099/00221287-44-2-149.

de Jong, B.W., Shi, S., Siewers, V., Nielsen, J., 2014. Improved production of fatty acid ethyl esters in *Saccharomyces cerevisiae* through up-regulation of the ethanol degradation pathway and expression of the heterologous phosphoketolase pathway. Microb. Cell Factories 13, 39. https://doi.org/10.1186/1475-2859-13-39.

Dele-Osibanjo, T., Li, Q., Zhang, X., Guo, X., Feng, J., Liu, J., Sun, X., Wang, X., Zhou, W., Zheng, P., Sun, J., Ma, Y., 2019. Growth-coupled evolution of phosphoketolase to improve l-glutamate production by *Corynebacterium glutamicum*. Appl. Microbiol. Biotechnol. 103, 8413–8425. https://doi.org/10.1007/s00253-019-10043-6.

Deutscher, D., Meilijson, I., Kupiec, M., Ruppin, E., 2006. Multiple knockout analysis of genetic robustness in the yeast metabolic network. Nat. Genet. 38, 993–998. https://doi.org/10.1038/ng1856.

Dijken, J.P., Scheffers, W.A., 1986. Redox balances in the metabolism of sugars by yeasts. FEMS Microbiol. Lett. 32, 199–224. https://doi.org/10.1111/j.1574-6968.1986.tb01194.x.

Entian, K.-D., Kötter, P., 2007. 25 yeast genetic strain and plasmid collections. In: Stansfield, I., Stark, M.J. (Eds.), Methods in Microbiology. Academic Press, pp. 629–666. https://doi.org/10.1016/S0580-9517(06)36025-4.

Ferreira, B.S., Calado, C.R.C., van Keulen, F., Fonseca, L.P., Cabral, J.M.S., da Fonseca, M.M.R., 2004. Recombinant *Saccharomyces cerevisiae* strain triggers acetate production to fuel biosynthetic pathways. J. Biotechnol. 109, 159–167. https://doi.org/10.1016/j.jbiotec.2003.10.033.

François, J.M., Lachaux, C., Morin, N., 2020. Synthetic biology applied to carbon conservative and carbon dioxide recycling pathways. Front. Bioeng. Biotechnol. 7, 1–16. https://doi.org/10.3389/fbioe.2019.00446.

Gietz, R.D., 2014. Yeast transformation by the LiAc/SS carrier DNA/PEG method. In: Methods in Molecular Biology, pp. 33–44. https://doi.org/10.1007/978-1-4939-0799-1_4.

Hoops, S., Sahle, S., Gauges, R., Lee, C., Pahle, J., Simus, N., Singhal, M., Xu, L., Mendes, P., Kummer, U., 2006. COPASI-a COmplex PAthway SImulator. Bioinformatics 22, 3067–3074. https://doi.org/10.1093/bioinformatics/btl485.

Hu, Y., Zhou, Y.J., Bao, J., Huang, L., Nielsen, J., Krivoruchko, A., 2017. Metabolic engineering of *Saccharomyces cerevisiae* for production of germacrene A, a precursor of beta-element. J. Ind. Microbiol. Biotechnol. 44, 1065–1072. https://doi.org/10.1007/s10295-017-1934-z.

Hügler, M., Menendez, C., Schägger, H., Fuchs, G., 2002. Malonyl-coenzyme a reductase from Chloroflexus aurantiacus, a key enzyme of the 3-hydroxypropionate cycle for autotrophic CO2 fixation. J. Bacteriol. 184, 2404–2410. https://doi.org/10.1128/JB.184.9.2404-2410.2002.

Inoue, H., Nojima, H., Okayama, H., 1990. High efficiency transformation of *Escherichia coli* with plasmids. Gene 96, 23–28. https://doi.org/10.1016/0378-1119(90)90336-P%20.

Jessop-Fabre, M.M., Jakočiūnas, T., Stovicek, V., Dai, Z., Jensen, M.K., Keasling, J.D., Borodina, I., 2016. EasyClone-MarkerFree: a vector toolkit for marker-less integration of genes into *Saccharomyces cerevisiae* via CRISPR-Cas9. Biotechnol. J. 11, 1110–1117. https://doi.org/10.1002/biot.201600147.

Kildegaard, K.R., Jensen, N.B., Schneider, K., Czarnotta, E., Özdemir, E., Klein, T., Maury, J., Ebert, B.E., Christensen, H.B., Chen, Y., Kim, I.K., Herrgård, M.J., Blank, L.M., Forster, J., Nielsen, J., Borodina, I., 2016. Engineering and systems-level analysis of Saccharomyces cerevisiae for production of 3-hydroxypropionic acid via malonyl-CoA reductase-dependent pathway. Microb. Cell Factories 15, 53. https://doi.org/10.1186/s12934-016-0451-5.

Kocharin, K., Siewers, V., Nielsen, J., 2013. Improved polyhydroxybutyrate production by *Saccharomyces cerevisiae* through the use of the phosphoketolase pathway. Biotechnol. Bioeng. 110, 2216–2224. https://doi.org/10.1002/bit.24888.

Kozak, B.U., van Rossum, H.M., Benjamin, K.R., Wu, L., Daran, J.-M.G., Pronk, J.T., van Maris, A.J.A., 2014a. Replacement of the *Saccharomyces cerevisiae* acetyl-CoA synthetases by alternative pathways for cytosolic acetyl-CoA synthesis. Metab. Eng. 21, 46–59. https://doi.org/10.1016/j.ymben.2013.11.005.

Kozak, B.U., van Rossum, H.M., Luttik, M.A.H., Akeroyd, M., Benjamin, K.R., Wu, L., de Vries, S., Daran, J.-M., Pronk, J.T., van Maris, A.J.A., 2014b. Engineering acetyl coenzyme A supply: functional expression of a bacterial pyruvate dehydrogenase complex in the cytosol of Saccharomyces cerevisiae. mBio 5. https://doi.org/10.1128/mBio.01696-14 e01696-14.

Krüsemann, J.L., Lindner, S.N., Dempfle, M., Widmer, J., Arrivault, S., Debacker, M., He, H., Kubis, A., Chayot, R., Anissimova, M., Marlière, P., Cotton, C.A.R., Bar-Even, A., 2018. Artificial pathway emergence in central metabolism from three recursive phosphoketolase reactions. FEBS J. 285, 4367–4377. https://doi.org/10.1111/febs.14682.

Lachaux, C., Frazao, C.J.R., Krauser, F., Morin, N., Walther, T., François, J.M., 2019. A new synthetic pathway for the bioproduction of glycolic acid from lignocellulosic sugars aimed at maximal carbon conservation. Front. Bioeng. Biotechnol. 7, 359. https://doi.org/10.3389/fbioe.2019.00359.

Lin, P.P., Jaeger, A.J., Wu, T.-Y., Xu, S.C., Lee, A.S., Gao, F., Chen, P.-W., Liao, J.C., 2018. Construction and evolution of an *Escherichia coli* strain relying on nonoxidative glycolysis for sugar catabolism. Proc. Natl. Acad. Sci. U.S.A. 115, 3538–3546. https://doi.org/10.1073/pnas.1802191115.

Lipmann, F., Tuttle, L.C., 1945. A specific micromethod for the determination of acyl phosphates. J. Biol. Chem. 159, 21–28.

Liu, Q., Yu, T., Li, X., Chen, Y., Campbell, K., Nielsen, J., Chen, Y., 2019. Rewiring carbon metabolism in yeast for high level production of aromatic chemicals. Nat. Commun. 10, 4976. https://doi.org/10.1038/s41467-019-12961-5.

Lynd, L.R., Wyman, C.E., Gerngross, T.U., 1999. Biocommodity engineering. Biotechnol. Prog. 15, 777–793. https://doi.org/10.1021/bp990109e.

Mans, R., van Rossum, H.M., Wijsman, M., Backx, A., Kuijpers, N.G.A., van den Broek, M., Daran-Lapujade, P., Pronk, J.T., van Maris, A.J.A., Daran, J.M.G., 2015. CRISPR/Cas9: a molecular Swiss army knife for simultaneous introduction of multiple genetic modifications in *Saccharomyces cerevisiae*. FEMS Yeast Res. 15, 1–15. https://doi.org/10.1093/femsyr/fov004.

Meadows, A.L., Hawkins, K.M., Tsegaye, Y., Antipov, E., Kim, Y., Raetz, L., Dahl, R.H., Tai, A., Mahatdejkul-Meadows, T., Xu, L., Zhao, L., Dasika, M.S., Murarka, A., Lenihan, J., Eng, D., Leng, J.S., Liu, C.-L., Wenger, J.W., Jiang, H., Chao, L., Westfall, P., Lai, J., Ganesan, S., Jackson, P., Mans, R., Platt, D., Reeves, C.D., Saija, P.R., Wichmann, G., Holmes, V.F., Benjamin, K., Hill, P.W., Gardner, T.S., Tsong, A.E., 2016. Rewriting yeast central carbon metabolism for industrial isoprenoid production. Nature 537, 694–697. https://doi.org/10.1038/nature19769.

Messiha, H.L., Kent, E., Malys, N., Carroll, K.M., Mendes, P., Smallbone, K., 2014. Enzyme characterisation and kinetic modelling of the pentose phosphate pathway in yeast. PeerJ Prepr 2, e146v4. https://doi.org/10.7287/peerj.preprints.146v1.

Nakahigashi, K., Toya, Y., Ishii, N., Soga, T., Hasegawa, M., Watanabe, H., Takai, Y., Honma, M., Mori, H., Tomita, M., 2009. Systematic phenome analysis of *Escherichia coli* multiple-knockout mutants reveals hidden reactions in central carbon metabolism. Mol. Syst. Biol. 5, 306. https://doi.org/10.1038/msb.2009.65.

Nielsen, J., 2014. Synthetic biology for engineering acetyl coenzyme a metabolism in yeast. mBio 5, 14–16. https://doi.org/10.1128/mBio.02153-14.

Nielsen, J., Jewett, M.C., 2008. Impact of systems biology on metabolic engineering of *Saccharomyces cerevisiae*. FEMS Yeast Res. 8, 122–131. https://doi.org/10.1111/j.1567-1364.2007.00302.x.

Nielsen, J., Keasling, J.D., 2016. Engineering cellular metabolism. Cell 164, 1185–1197. https://doi.org/10.1016/j.cell.2016.02.004.

Racker, E., 1962. Fructose-6-phosphate phosphoketolase from *Acetobacter xylinum*. Methods Enzymol. 5, 276–280. https://doi.org/10.1016/S0076-6879(62)05219-2.

Ramos, J., Sychrová, H., Kschischo, M., 2016. Yeast membrane transport. In: Ramos, J., Sychrová, H., Kschischo, M. (Eds.), Yeast Membrane Transporter, Advances in Experimental Medicine and Biology. Springer International Publishing, Cham. https://doi.org/10.1007/978-3-319-25304-6, 299–51.

Rodriguez, A., Kildegaard, K.R., Li, M., Borodina, I., Nielsen, J., 2015. Establishment of a yeast platform strain for production of p-coumaric acid through metabolic engineering of aromatic amino acid biosynthesis. Metab. Eng. 31, 181–188. https://doi.org/10.1016/J.YMBEN.2015.08.003.

Schaaff-Gerstenschläger, I., Mannhaupt, G., Vetter, I., Zimmermann, F.K., Feldmann, H., 1993. *TKL2*, a second transketolase gene of *Saccharomyces cerevisiae*. Eur. J. Biochem. 217, 487–492. https://doi.org/10.1111/j.1432-1033.1993.tb18268.x.

Schramm, M., Racker, E., 1957. Formation of erythrose-4-phosphate and acetyl phosphate by a phosphorolytic cleavage of fructose-6-phosphate. Nature. https://doi.org/10.1038/1791349a0.

Shi, S., Chen, Y., Siewers, V., Nielsen, J., 2014. Improving production of malonyl coenzyme A-derived metabolites by abolishing snf1-dependent regulation of Acc1. mBio 5. https://doi.org/10.1128/mbio.01130-14.

Smallbone, K., Messiha, H.L., Carroll, K.M., Winder, C.L., Malys, N., Dunn, W.B., Murabito, E., Swainston, N., Dada, J.O., Khan, F., Pir, P., Simeonidis, E., Spasić, I., Wishart, J., Weichart, D., Hayes, N.W., Jameson, D., Broomhead, D.S., Oliver, S.G., Gaskell, S.J., McCarthy, J.E.G., Paton, N.W., Westerhoff, H.V., Kell, D.B., Mendes, P., 2013. A model of yeast glycolysis based on a consistent kinetic characterisation of all its enzymes. FEBS Lett. 587, 2832–2841. https://doi.org/10.1016/j.febslet.2013.06.043.

Suzuki, R., Katayama, T., Kim, B.-J., Wakagi, T., Shoun, H., Ashida, H., Yamamoto, K., Fushinobu, S., 2010. Crystal structures of phosphoketolase: thiamine diphosphate-dependent dehydration mechanism. J. Biol. Chem. 285, 34279–34287. https://doi.org/10.1074/jbc.M110.156281.

Swinnen, S., Klein, M., Carrillo, M., McInnes, J., Nguyen, H.T., Nevoigt, E., 2013. Re-evaluation of glycerol utilization in *Saccharomyces cerevisiae*: characterization of an isolate that grows on glycerol without supporting supplements. Biotechnol. Biofuels 6, 157. https://doi.org/10.1186/1754-6834-6-157.

Teusink, B., Passarge, J., Reijenga, C.A., Esgalhado, E., van der Weijden, C.C., Schepper, M., Walsh, M.C., Bakker, B.M., van Dam, K., Westerhoff, H.V., Snoep, J.L., 2000. Can yeast glycolysis be understood in terms of *in vitro* kinetics of the constituent enzymes? Testing biochemistry. Eur. J. Biochem. 267, 5313–5329. https://doi.org/10.1046/j.1432-1327.2000.01527.x.

van Dijken, J., Bauer, J., Brambilla, L., Duboc, P., Francois, J., Gancedo, C., Giuseppin, M.L., Heijnen, J., Hoare, M., Lange, H., Madden, E., Niederberger, P., Nielsen, J., Parrou, J., Petit, T., Porro, D., Reuss, M., van Riel, N., Rizzi, M., Steensma, H., Verrips, C., Vindeløv, J., Pronk, J., 2000. An interlaboratory comparison of physiological and genetic properties of four *Saccharomyces cerevisiae* strains. Enzym. Microb. Technol. 26, 706–714. https://doi.org/10.1016/S0141-0229(00)00162-9.

van Rossum, H.M., Kozak, B.U., Pronk, J.T., van Maris, A.J.A., 2016. Engineering cytosolic acetyl-coenzyme A supply in *Saccharomyces cerevisiae*: pathway stoichiometry, free-energy conservation and redox-cofactor balancing. Metab. Eng. 36, 99–115. https://doi.org/10.1016/j.ymben.2016.03.006.

Verduyn, C., Postma, E., Scheffers, W.A., van Dijken, J.P., 1992. Effect of benzoic acid on metabolic fluxes in yeasts: respiration and alcoholic fermentation. Yeast 8, 501–517. https://doi.org/10.1007/BF00270792.

Wang, Q., Xu, J., Sun, Z., Luan, Y., Li, Y., Wang, J., Liang, Q., Qi, Q., 2019. Engineering an *in vivo* EP-bifido pathway in *Escherichia coli* for high-yield acetyl-CoA generation with low CO2 emission. Metab. Eng. 51, 79–87. https://doi.org/10.1016/j.ymben.2018.08.003.

Weinhandl, K., Winkler, M., Glieder, A., Camattari, A., 2014. Carbon source dependent promoters in yeasts. Microb. Cell Factories 13, 5. https://doi.org/10.1186/1475-2859-13-5.

Woolston, B.M., King, J.R., Reiter, M., Van Hove, B., Stephanopoulos, G., 2018. Improving formaldehyde consumption drives methanol assimilation in engineered *E. coli*. Nat. Commun. 9, 2387. https://doi.org/10.1038/s41467-018-04795-4.

Xu, H., Kim, S., Sorek, H., Lee, Y., Jeong, D., Kim, J., Oh, E.J., Yun, E.J., Wemmer, D.E., Kim, K.H., Kim, S.R., Jin, Y.S., 2016. *PHO13* deletion-induced transcriptional activation prevents sedoheptulose accumulation during xylose metabolism in engineered *Saccharomyces cerevisiae*. Metab. Eng. 34, 88–96. https://doi.org/10.1016/j.ymben.2015.12.007.

Yang, X., Yuan, Q., Zheng, Y., Ma, H., Chen, T., Zhao, X., 2016. An engineered non-oxidative glycolysis pathway for acetone production in *Escherichia coli*. Biotechnol. Lett. 38, 1359–1365. https://doi.org/10.1007/s10529-016-2115-2.

Yu, T., Zhou, Y.J., Huang, M., Liu, Q., Pereira, R., David, F., Nielsen, J., 2018. Reprogramming yeast metabolism from alcoholic fermentation to lipogenesis. Cell 174, 1549–1558. https://doi.org/10.1016/j.cell.2018.07.013 e14.

Zhou, Y.J., Gao, W., Rong, Q., Jin, G., Chu, H., Liu, W., Yang, W., Zhu, Z., Li, G., Zhu, G., Huang, L., Zhao, Z.K., 2012. Modular pathway engineering of diterpenoid synthases and the mevalonic acid pathway for miltiradiene production. J. Am. Chem. Soc. 134, 3234–3241. https://doi.org/10.1021/ja2114486.

Zhu, Z., Hu, Y., Teixeira, P.G., Pereira, R., Chen, Y., Siewers, V., Nielsen, J., 2020. Multidimensional engineering of *Saccharomyces cerevisiae* for efficient synthesis of medium-chain fatty acids. Nat. Catal. 3, 64–74. https://doi.org/10.1038/s41929-019-0409-1.